



Cite this: *Chem. Commun.*, 2018, 54, 13945

Received 18th October 2018,  
Accepted 13th November 2018

DOI: 10.1039/c8cc08341j

rsc.li/chemcomm

## Reversible redox inter-conversion of biologically active NAD<sup>+</sup>/NADH derivatives bound to a gold electrode: ToF-SIMS evidence†

Ruo-Can Qian,<sup>‡</sup> Li-Jun Zhao,<sup>‡</sup> Jian Lv, Xin Hua<sup>‡</sup> and Yi-Tao Long<sup>‡\*</sup>

**The realization of the reversible inter-conversion between NADH and NAD<sup>+</sup> is a long-term challenge in biological and energy-related chemistry. Here, we achieve the electrochemical reversible redox of NAD<sup>+</sup>/NADH derivatives by the functionalization of a gold electrode with a specially designed NAD<sup>+</sup> derivative, and the electrochemical redox products are characterized by time-of-flight secondary ion mass spectrometry (ToF-SIMS).**

As a ubiquitous biomolecule in all living cells, nicotinamide adenine dinucleotide (NAD<sup>+</sup>) is involved in many important energy and electron transport processes.<sup>1</sup> However, researchers are still plagued by the irreversible inter-conversion during the electrochemical redox of NAD<sup>+</sup>.<sup>2</sup> Previous studies indicate that two steps may be involved in the electrochemical reduction of NAD<sup>+</sup>. In the first step, NAD<sup>+</sup> is reduced to NAD<sup>•+</sup> radicals, which is the rate-determining step. In the second step, the generated NAD<sup>•+</sup> radicals could be converted into two different reduction products (an inactive dimer NAD<sub>2</sub> and enzymatically-active NADH) by different ways. Meanwhile, the formation of dimer NAD<sub>2</sub> is far faster than the generation of NADH, and the enzymatically-active NADH could hardly be regenerated during NAD<sup>+</sup> electrochemical reduction.<sup>3</sup>

To date, only a few strategies have been proven to be effective for the electrochemically reversible inter-conversion of NAD<sup>+</sup>/NADH. In a recent work, a ubiquinone mediated hybrid lipid bilayer membrane system is used to realize the electrochemically reversible interconversion between NADH and NAD<sup>+</sup>.<sup>4</sup> Another research work reported the use of a liquid crystal membrane electrode to regenerate enzymatically active NADH from NAD<sup>+</sup>.<sup>5</sup> In addition, the redox inter-conversion between NAD<sup>+</sup> and NADH can also be easily realized *in vivo*, and the standard potential is −0.56 V vs. saturated calomel electrode (SCE).<sup>3</sup> Although the electrochemical redox inter-conversion of

NAD<sup>+</sup>/NADH has been successfully implemented, the construction of these biomimetic membrane systems is still rather complex and instable. Therefore, there is an urgent need to explore more simple and stable systems to realize the inter-conversion of NAD<sup>+</sup>/NADH.

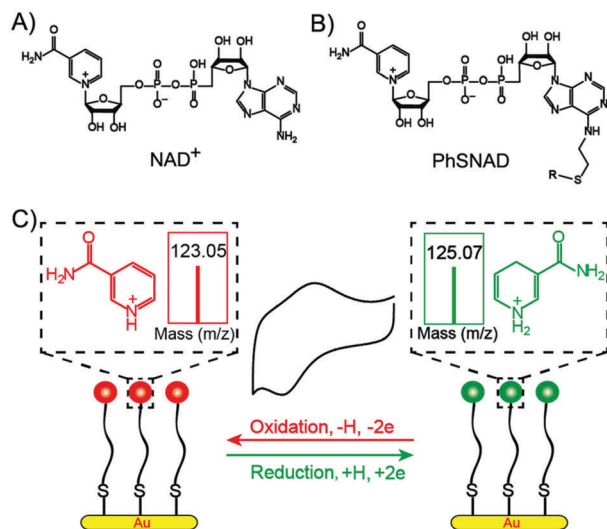
In the past research studies, the electrochemical behaviors of various redox electroactive molecules on electrode surfaces have been explored and shown to present favourable properties in electrocatalysis, molecular scale devices, battery electrodes and electrochemical analysis and so on.<sup>6</sup> However, the electrochemical research of NAD<sup>+</sup> on the electrode surface is still underexplored due to the complex structure modification of NAD<sup>+</sup> molecules and unfavorable surface analysis techniques. Due to the far reaching application potential of the ToF-SIMS surface analysis technique in the field of molecular analysis,<sup>7</sup> we are inspired to explore the surface electrochemical behaviour of NAD<sup>+</sup> with the help of ToF-SIMS.

In this work, we focused on the electrochemical research studies of NAD<sup>+</sup> molecules on the surface of gold electrodes based on electrochemical surface analysis and the ToF-SIMS technique, which enabled the realization of the electrochemically reversible inter-conversion of NAD<sup>+</sup>/NADH. A special benzyl sulfide functionalized NAD<sup>+</sup> derivative, PhSNAD, was designed and used for the modification of the gold electrode. The benzyl sulfide group modified on the C-6 of the adenine ring was beneficial for the conjugation of the PhSNAD molecules to the gold electrode surface with little effect on the biological activities of natural NAD<sup>+</sup>.<sup>8</sup> As shown in Scheme 1, the PhSNAD molecules were locked on the surface of gold electrode. Therefore, the intermediate products of electrochemical reduction, NAD<sup>•+</sup> radicals, would then transform to the enzymatically active NADH instead of the inactive dimer NAD<sub>2</sub>. By analysing the electrochemical redox products of NAD<sup>+</sup> on the electrode surface, related characteristic fragment ions of the NADH and NAD<sup>+</sup> were observed, demonstrating the reversible inter-conversion of the NAD<sup>+</sup>/NADH derivatives. This approach to modify PhSNAD molecules on the gold electrode surface allows for the reversible inter-conversion of NAD<sup>+</sup>/NADH and the development of a new convenient tool for the study of NAD<sup>+</sup>/NADH-evolved biopathways.

Key Laboratory for Advanced Materials, School of Chemistry & Molecular Engineering, East China University of Science and Technology, 130 Meilong Road, Shanghai, 200237, P. R. China. E-mail: yitlong@ecust.edu.cn

† Electronic supplementary information (ESI) available: Detailed description of the materials and experimental. See DOI: 10.1039/c8cc08341j

‡ These authors contributed equally to this work.



**Scheme 1** The molecular structures of (A)  $\text{NAD}^+$  and (B) PhSNAD. (C) Schematic illustration of the PhSNAD modified electrode and electrochemically reversible redox of  $\text{NAD}^+$  on the electrode surface.

According to the previous studies, the electrochemical activity of the thiol  $\text{NAD}^+$  derivative (substituted on the C-6 of the adenine ring) is mainly from the nicotinamide part, and its electrochemical activity in solution is similar to that of natural  $\text{NAD}^+$ .<sup>9</sup> Here a novel  $\text{NAD}^+$  derivative, PhSNAD, was synthesized by modifying the C-6 with benzyl sulfide for the modification of the gold electrode. Fig. S1 (ESI<sup>†</sup>) shows the synthetic procedure of PhSNAD. Benzyl mercaptan was treated with 2-chloroethylamine hydrochloride in the presence of sodium ethoxide to give a primary amine b-2 by a Friedel-Crafts type condensation reaction.<sup>10</sup> The benzyl sulfide-modified adenine nucleotide d-2 was prepared by the condensation of the resulting primary amine b-2 with the adenine nucleotide d-1.<sup>11</sup> Then the benzyl sulfide-modified adenine nucleotide d-2 was phosphorylated with  $\text{POCl}_3$  to give a vitamin B8 derivative d-3. The generated vitamin B8 derivative d-3 was further activated with morpholine to give d-4, which was then coupled with nicotinamide mononucleotide  $\beta\text{-NMN}^+$  to afford PhSNAD.<sup>12</sup> All compounds were characterized by  $^1\text{H}$  NMR,  $^{13}\text{C}$  NMR and mass spectroscopy, and the compounds d-3, d-4 and PhSNAD were also characterized by  $^{31}\text{P}$  NMR.

The coenzyme activity of the synthetic compound PhSNAD was firstly investigated by UV-vis spectroscopy. A typical enzymatic oxidation of ethanol to acetaldehyde catalyzed by alcohol dehydrogenases (ADH) was used to assess the coenzyme activity of PhSNAD.<sup>13</sup> After the addition of PhSNAD, the intensity of the absorption peak at 267 nm decreased while that of the peak at 340 nm increased with the incubation time (Fig. 1A), which was similar to the situation in the presence of  $\text{NAD}^+$  (Fig. 1B). The above results demonstrated the excellent coenzyme activities of PhSNAD. Thus, the designed PhSNAD was perfectly suitable for researching the superficial electrochemical redox process and mechanism of  $\text{NAD}^+$ .

The CVs of compound PhSNAD were firstly investigated in PBS (0.1 M, pH 7.0) with glassy carbon (GC) electrodes (3 mm in diameter). As shown in Fig. 2, the reduction potential

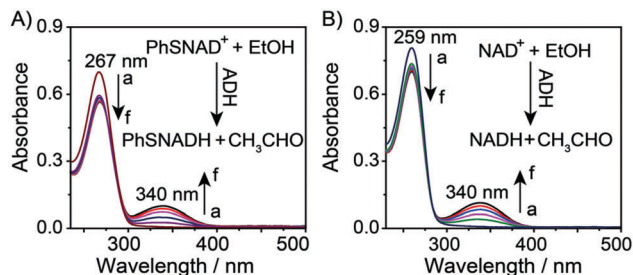


**Fig. 1** UV-vis spectra of PhSNAD (A) or  $\text{NAD}^+$  standard (B) after incubation with alcohol dehydrogenase (ADH) in the presence of ethanol at 25 °C for 0 min (a), 5 min (b), 10 min (c), 15 min (d), 20 min (e) and 30 min (f).

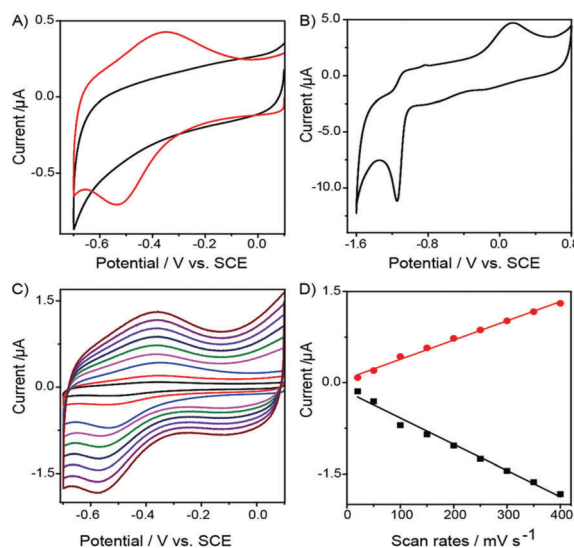


**Fig. 2** (A) CVs of the PhSNAD modified electrode in PBS (0.1 M, pH 7.4). (B) CVs of the bare GC electrodes in PBS (0.1 M, pH 7.4) containing 1 mM PhSNAD. Scan rates: 100  $\text{mV s}^{-1}$ . (C) Relationships of peak currents with scan rates: 20, 50, 100, 150, 200, 250, 300, 350 and 400  $\text{mV s}^{-1}$ . (D) Linear relationships were determined to be:  $y = 0.0030x + 0.0670$ ,  $R = 0.9939$ ;  $y = -0.0040x - 0.1506$ ,  $R = 0.9973$ , respectively.

and oxidation potential of PhSNAD were determined to be  $-1.15$  V and  $0.14$  V, respectively. Under the same conditions, the reduction potential and oxidation potential of  $\text{NAD}$  were measured to be  $-1.13$  V and  $0.12$  V, respectively (Fig. S2, ESI<sup>†</sup>). Thus, the synthetic PhSNAD showed similar electrochemical properties to those of  $\text{NAD}$ .

Nevertheless, significant overpotentials still existed, which are 0.5 V for the anodic peak and 0.8 V for the cathodic peak, respectively. As mentioned previously, these overpotentials were mainly attributed to the formation of the  $\text{NAD}^+$  dimer during the reduction of  $\text{NAD}^+$  to  $\text{NADH}$  in the solution state. In this case, next we investigated the electrochemical behaviours of PhSNAD fixed on the surface of a gold electrode.

In order to research the electrochemical behaviours of  $\text{NAD}^+$  on the surface of the electrode, a  $\text{NAD}^+$  modified electrode was prepared and characterized by X-ray photoelectron spectroscopy (XPS) and ToF-SIMS, respectively. The elements change in the XPS spectra of the electrode surface after PhSNAD modification, which confirmed the successful modification of the  $\text{NAD}^+$

molecules on the gold electrode (Fig. S3, ESI<sup>†</sup>). Importantly, from the ToF-SIMS spectra, we further investigated the modification of NAD<sup>+</sup> on the electrode surface with direct evidence. As shown in Fig. S4 (ESI<sup>†</sup>), the ToF-SIMS spectra of the gold electrodes showed significant changes before and after the modification of NAD<sup>+</sup>. For the bare gold electrode, the ToF-SIMS spectra showed no characteristic ion peaks of NAD<sup>+</sup> except some background signals of gold (Fig. S4A, ESI<sup>†</sup>). After NAD<sup>+</sup> modification, several characteristic ion peaks of NAD<sup>+</sup> were observed at 814.16 (Fig. S4B-a, ESI<sup>†</sup>), 135.16 and 136.16 (Fig. S4B-b, ESI<sup>†</sup>) and 123.05 (Fig. S4B-c, ESI<sup>†</sup>), respectively. Among these characteristic ion peaks, the peak at 814.16 is attributed to the molecular ions [M + H]<sup>+</sup> of PhSNAD; the peaks at 135.16 and 136.16 could be assigned to the nicotinamide fragment ions [M]<sup>+</sup> and [M + H]<sup>+</sup>; and the peak at 123.05 could be assigned to the nicotinamide fragment ion [M]<sup>+</sup>, respectively. Moreover, a control experiment was also performed using a pure PhSNAD coated silicon wafer, which showed the same characteristic ion peaks at 814.16 (Fig. S4C-a, ESI<sup>†</sup>), 135.16 and 136.16 (Fig. S4C-b, ESI<sup>†</sup>), and 123.05 (Fig. S4C-c, ESI<sup>†</sup>), demonstrating the fabrication of NAD<sup>+</sup> modified electrodes.

The CVs of the NAD<sup>+</sup> modified electrodes were recorded in pH 7.0 PBS (38 mL 0.1 M NaH<sub>2</sub>PO<sub>4</sub>, 62 mL Na<sub>2</sub>HPO<sub>4</sub>). As shown in Fig. 2A, a couple of redox peaks were observed at a lower potential, and the oxidation potential and reduction potential were -0.53 V and -0.35 V, respectively. The surface coverage ( $\Gamma$ , mol cm<sup>-2</sup>) of NAD<sup>+</sup> was calculated to be  $\sim 1.64 \times 10^{-10}$  mol cm<sup>-2</sup> using the integrated charge ( $Q$ ) of both cathodic and anodic peaks according to eqn (1),

$$\Gamma = Q/nFA \quad (1)$$

where  $n$  is the number of electrons exchanged per NAD<sup>+</sup> molecule (considering the two-electron process for the NAD<sup>+</sup>/NADH couple,  $n = 2$ ),  $A$  is the area of the electrode and  $F$  is the Faraday constant. The result was consistent with a theoretical coverage of  $1.68 \times 10^{-10}$  mol cm<sup>-2</sup>, obtained according to the size of the PhSNAD molecules and the areas of the electrodes.<sup>14</sup> Furthermore, the relation between the Faradaic peak current and the scan rate was investigated. As demonstrated in Fig. 2B, the Faradaic peak current was proportional to the scan rate, suggesting an adsorption controlled electrode process. In addition, the redox

peaks of NAD<sup>+</sup> reached a stable state after cycling from 0.1 to -0.7 V for 20 sweeps (Fig. S5, ESI<sup>†</sup>), which indicated the good stability of the NAD<sup>+</sup> modified electrodes. According to the previous hypothesis explaining the electrochemical reaction mechanism of NAD<sup>+</sup> molecules in solutions, when the NAD<sup>+</sup> molecules are immobilized on the surface of electrodes, the formation of NAD<sup>+</sup> dimer will be blocked, thus inducing the formation of enzymatically-active NADH from the NAD<sup>+</sup> radicals. Therefore, we deduced that the obtained CV redox peaks were probably attributed to the NAD<sup>+</sup>/NADH derivative redox couple.

To determine the corresponding electrochemical redox products, ToF-SIMS was used to further monitor the surface changes of the NAD<sup>+</sup> electrodes during the CV experiment. As shown in Fig. 3A (inset), there were no obvious ion peak observed for the bare gold electrode in the range of 120 to 130. However, the characteristic fragment ions of NAD<sup>+</sup> were observed at 123.05 after modifying the electrode with NAD<sup>+</sup> (Fig. 3A), which could be assigned to the nicotinamide fragment ion [M]<sup>+</sup> as described above. The ToF-SIMS spectrum of the NAD<sup>+</sup> standard on the surface of a silicon wafer was also analysed, and the same fragment ion peak of the nicotinamide fragment ion [M]<sup>+</sup> was acquired at 123.05 (Fig. 3C, inset), which confirmed that the fragment ion peak in Fig. 3A was from the nicotinamide part. After reducing the NAD<sup>+</sup> modified electrode at -0.6 V for 5 min, the ToF-SIMS spectrum showed that the nicotinamide fragment ion peak at 123.05 disappeared and a new ion peak appeared at 125.07 (Fig. 3B). We deduced that the new ion peak was from the generated NADH at the surface of the electrode. Compared with NAD<sup>+</sup>, one hydrogen proton was added in position 4 of the pyridine ring and the positively charged nitrogen was transformed into a neutral nitrogen atom for NADH. In the positive ion mode, the new fragment ion peak at 125.07 could be attributed to the reduced nicotinamide part from the regenerated NADH. In order to further test the above deduction, the ToF-SIMS spectrum of the NADH standard on the surface of a cleaning silicon wafer was also analysed (Fig. 3B, inset). The same characteristic peak of the reduced nicotinamide was acquired, which demonstrated the generation of NADH during the electrochemical reduction of NAD<sup>+</sup> on the electrode surface.

To prove the reversible properties of NAD<sup>+</sup> electrochemical redox on the surface of the electrode, the modified gold electrode

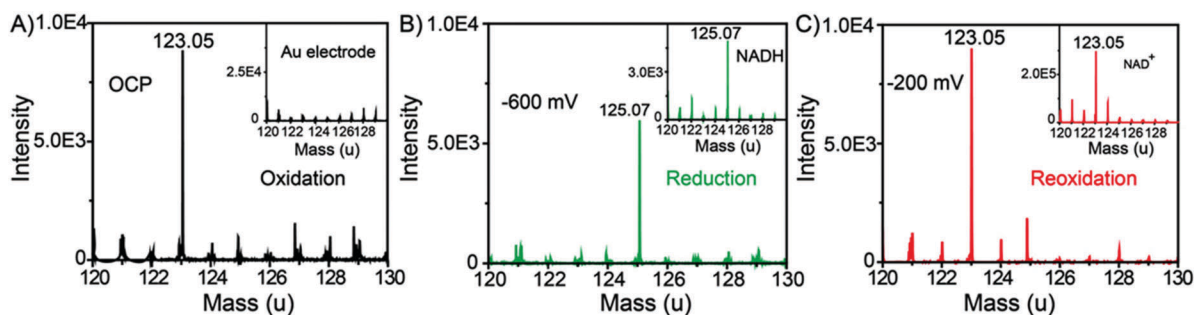


Fig. 3 The redox products of the PhSNAD modified electrodes monitored by TOF-SIMS with Bi<sub>3</sub><sup>++</sup> primary ion beams. (A) Open circuit potential (OCP), inset: TOF-SIMS spectrum of the bare gold electrodes; (B) an applied potential of -0.60 V vs. SCE, inset: TOF-SIMS spectrum of the commercial NADH coated silicon wafer; (C) an applied potential of -0.20 V vs. SCE, inset: TOF-SIMS spectrum of the commercial NAD<sup>+</sup> coated silicon wafer.

was then electrochemically oxidized at  $-0.2$  V for 5 min. By ToF-SIMS analysis, we found that the ion peak at 125.07 sharply decreased and the ion peak at 123.05 reappeared (Fig. 3C), which demonstrated that the generated NADH was reoxidized to  $\text{NAD}^+$  on the surface of the electrode. In addition, a controlled experiment was performed using the  $\text{NAD}^+$  dimer. As shown in Fig. S6 (ESI<sup>†</sup>), the ToF-SIMS spectrum of the  $\text{NAD}^+$  dimer was recorded, and a significant special peak of the  $\text{NAD}^+$  dimer was observed at 269.04. The characteristic peak at 269.04 could be attributed to the reduced nicotinamide dimer part from the  $\text{NAD}^+$  dimer, which demonstrated that the generation of a  $\text{NAD}^+$  dimer was successfully blocked in this system. Thus, an electrochemically reversible redox of  $\text{NAD}^+/\text{NADH}$  derivatives was realized on the electrode surface.

For the generated NADH on the surface of the electrode, we also investigated its coenzyme activity for ADH. Generally, ADH could catalyze the reduction of acetaldehyde to ethanol in the presence of NADH, which is oxidized to  $\text{NAD}^+$ .<sup>15</sup> Here, we performed an enzymatic experiment of the electrochemically generated NADH by immersing the reduced  $\text{NAD}^+$  derivative modified electrodes in a mixture of acetaldehyde and ADH. Thus the enzymatic triggered changes of  $\text{NADH}/\text{NAD}^+$  could be monitored by ToF-SIMS. As described above, a typical fragment ion peak was detected at 125.07 for the reduced  $\text{NAD}^+$  derivative modified electrodes (Fig. 3B). However, after incubating the reduced  $\text{NAD}^+$  modified electrodes in the mixture solution of acetaldehyde and ADH at  $37^\circ\text{C}$  for 30 min, the fragment ion peak of NADH significantly degraded and another typical fragment ion peak of  $\text{NAD}^+$  emerged at 123.05 (Fig. S7, ESI<sup>†</sup>), demonstrating that the generated NADH maintained favorable coenzyme activity.<sup>16</sup>

In conclusion, we have synthesized a special benzyl sulfide-modified  $\text{NAD}^+$  derivative, PhSNAD, and realized the electrochemically reversible inter-conversion between NADH and  $\text{NAD}^+$  using  $\text{NAD}^+$  derivative modified electrodes. The CVs of the  $\text{NAD}^+$  modified gold electrode shows a couple of quasi-reversible redox peaks, demonstrating the reversible inter-conversion of the  $\text{NAD}^+/\text{NADH}$  derivatives. In addition, we monitored the corresponding electrochemical redox products of the  $\text{NAD}^+$  molecules modified on the surface of the electrode and researched the enzymatic activity of the regenerated NADH on the surface of the electrode using ToF-SIMS. Therefore, this work provides a different method to monitor the electrochemically reversible redox of  $\text{NAD}^+/\text{NADH}$  derivatives simultaneously on an electrode surface, showing great potential for the further investigation of  $\text{NAD}^+/\text{NADH}$ -evolved biopathways.

This research was supported by the National Natural Science Foundation of China (21421004, 21327807, 21605048), the Program of Introducing Talents of Discipline to Universities (B16017), the Innovation Program of Shanghai Municipal Education Commission (2017-01-07-00-02-E00023), the Fundamental Research Funds for the Central Universities (222201718001, 222201717003), the Chenguang Program (16CG35), and the Shanghai Education Development Foundation and the Shanghai Municipal Education Commission.

## Conflicts of interest

There are no conflicts to declare.

## Notes and references

- (a) A. Schmid, J. S. Dordick, B. Hauer, A. Kiener, M. Wubolts and B. Witholt, *Nature*, 2001, **409**, 258–268; (b) N. Simpson, D. J. Shaw, P. W. J. M. Frederix, A. H. Gillies, K. Adamczyk, G. M. Greetham, M. Towrie, A. W. Parker, P. A. Hoskisson and N. T. Hunt, *J. Phys. Chem. B*, 2013, **117**, 16468–16478; (c) N. D. Rose and J. M. Regan, *Bioelectrochemistry*, 2015, **106**, 213–220.
- (a) F. M. Maddar, R. A. Lazenby, A. N. Patel and P. R. Unwin, *Phys. Chem. Chem. Phys.*, 2016, **18**, 26404–26411; (b) H. Shuo, J. B. Zhang, X. Y. Gao and H. Y. Ying, *J. Mater. Chem. B*, 2015, **3**, 6626–6633; (c) S. Shipovskov, A. Bonamore, A. Boffi and E. E. Ferapontova, *Chem. Commun.*, 2015, **51**, 16096–16098; (d) B. Siritanaratkul, C. F. Megarity, T. G. Roberts, T. O. Samuels, M. Winkler, J. H. Warner, T. Happe and F. A. Armstrong, *Chem. Sci.*, 2017, **8**, 4579–4586; (e) J. Moiroux and P. J. Elving, *J. Electroanal. Chem.*, 1979, **102**, 93–108.
- (a) N. Ullah, I. Ali and S. Omanovic, *Mater. Chem. Phys.*, 2015, **149–150**, 413–417; (b) L. Gorton and E. Dominguez, *Electrochemistry of  $\text{NAD(P)}^+/\text{NAD(P)H}$* , Wiley-VCH Verlag GmbH & Co, KGaA, 2007, **3**, 389–394.
- W. Ma, D. W. Li, T. C. Sutherland, Y. Li, Y. T. Long and H. Y. Chen, *J. Am. Chem. Soc.*, 2011, **133**, 12366–12369.
- C. H. Wong, L. Daniels, W. H. Orme-Johnson and G. M. Whitesides, *J. Am. Chem. Soc.*, 1981, **103**, 6227–6228.
- (a) T. Zhang, Z. Ma, L. Wang, J. Xi and Z. Shuai, *Philos. Trans. R. Soc. London*, 2014, **372**, 20130018; (b) S. Tsoi, I. Griva, S. A. Trammell, A. S. Blum, J. M. Schnur and N. Lebedev, *ACS Nano*, 2008, **2**, 1289–1295; (c) L. B. Zhao, M. Zhang, B. Ren, Z. Q. Tian and D. Y. Wu, *J. Phys. Chem. C*, 2014, **118**, 27113–27122; (d) V. Radu, S. Frielingsdorf, S. D. Evans, O. Lenz and L. J. C. Jeuken, *J. Am. Chem. Soc.*, 2014, **136**, 8512–8515; (e) C. J. Barile, E. C. M. Tse, Y. Li, T. B. Sobyra, S. C. Zimmerman, A. Hosseini and A. A. Gewirth, *Nat. Mater.*, 2014, **13**, 619–623.
- (a) H. Lee, S. M. Dellatore, W. M. Miller and P. B. Messersmith, *Science*, 2007, **318**, 426–430; (b) H. Gu, Z. Yang, J. Gao, C. K. Chang and B. Xu, *J. Am. Chem. Soc.*, 2005, **127**, 34–35; (c) C. W. T. Bulle-Lieuwma, W. J. H. van Gennip, J. K. J. van Duren, P. Jonkheijm, R. A. J. Janssen and J. W. Niemantsverdriet, *Appl. Surf. Sci.*, 2003, **203–204**, 547–550; (d) J. S. Fletcher and J. C. Vickerman, *Anal. Chem.*, 2013, **85**, 610–639; (e) J. Bailey, R. Havelund, A. G. Shard, I. S. Gilmore, M. R. Alexander, J. S. Sharp and D. J. Scurr, *ACS Appl. Mater. Interfaces*, 2015, **7**, 2654–2659; (f) P. Totaro, L. Poggini, A. Favre, M. Mannini, P. Saintavit, A. Cornia, A. Magnani and R. Sessoli, *Langmuir*, 2014, **30**, 8645–8649.
- D. O. Bellisario, A. D. Jewell, H. L. Tierney, A. E. Baber and E. C. H. Sykes, *J. Phys. Chem. C*, 2010, **114**, 14583–14589.
- (a) J. Lee, H. Churchil, W. B. Choi, J. E. Lynch, F. E. Roberts, R. P. Volante and P. J. Reider, *Chem. Commun.*, 1999, 729–730; (b) N. E. Batoux, F. Paradisi, P. C. Engel and M. E. Migaud, *Tetrahedron*, 2004, **60**, 6609–6617; (c) B. Zhang, G. K. Wagner, K. Weber, C. Garnham, A. J. Morgan, A. Galione, A. H. Guse and B. V. L. Potter, *J. Med. Chem.*, 2008, **51**, 1623–1636; (d) C. Moreau, T. Kirchberger, B. Zhang, M. P. Thomas, K. Weber, A. H. Guse and B. V. L. Potter, *J. Med. Chem.*, 2012, **55**, 1478–1489; (e) H. Jiang, J. Congleton, Q. Liu, P. Merchant, F. Malavasi, H. C. Lee, Q. Hao, A. Yen and H. Lin, *J. Am. Chem. Soc.*, 2009, **131**, 1658–1659; (f) H. Jiang, J. H. Kim, K. M. Frizzell, W. L. Kraus and H. Lin, *J. Am. Chem. Soc.*, 2010, **132**, 9363–9372.
- N. Boden, R. J. Bushby, S. Clarkson, S. D. Evans, P. F. Knowles and A. Marsh, *Tetrahedron*, 1997, **53**, 10939–10952.
- T. D. Ashton, S. P. Baker, S. A. Hutchinson and P. J. Scammells, *Biorg. Med. Chem.*, 2008, **16**, 1861–1873.
- C. Moreau, G. K. Wagner, K. Weber, A. H. Guse and B. V. L. Potter, *J. Med. Chem.*, 2006, **49**, 5162–5176.
- A. A. Heikal, *Biomarkers Med.*, 2010, **4**, 241–263.
- N. V. Rees, Y. G. Zhou and R. G. Compton, *Chem. Phys. Lett.*, 2012, **525–526**, 69–71.
- (a) W. Gao, Y. Chen, J. Xi, S. Lin, Y. Chen, Y. Lin and Z. Chen, *Biosens. Bioelectron.*, 2013, **41**, 776–782; (b) X. Wang, L. Li, Y. Wang, C. Xu, B. Zhao and X. Yang, *Food Chem.*, 2013, **138**, 2195–2200.
- (a) S. Hayward and A. Kitao, *Biophys. J.*, 2006, **91**, 1823–1831; (b) V. Flexer, F. Durand, S. Tsujimura and N. Mano, *Anal. Chem.*, 2011, **83**, 5721–5727.